Review

Advances in electrocatalysts for oxygen evolution reaction of water electrolysis-from metal oxides to carbon nanotubes

Yi Cheng, San Ping Jiang[*]

Fuels and Energy Technology Institute & Department of Chemical Engineering, Curtin University, Perth, WA 6102, Australia

Abstract

The water electrolysis for hydrogen production is constrained by the thermodynamically unfavorable oxygen evolution reaction (OER), which requires input of a large amount of energy to drive the reaction. One of the key challenges to increase the efficiency of the water electrolysis system is to develop highly effective and robust electrocatalysts for the OER. In the past 20–30 years, significant progresses have been made in the development of efficient electrocatalysts, including metal oxides, metal oxide-carbon nanotubes (CNTs) hybrid and metal-free CNTs based materials for the OER. In this critical review, the overall progress of metal oxides catalysts and the role of CNTs in the development of OER catalyst are summarized, and the latest development of new metal free CNTs-based OER catalyst is discussed.
© 2015 The Authors. Production and hosting by Elsevier B.V. on behalf of Chinese Materials Research Society. This is an open access article under the CC BY-NC-ND license (http://creativecommons.org/licenses/by-nc-nd/4.0/).

Keywords: Water electrolysis; Oxygen reduction reaction; Metal oxide; Hybrid metal oxide/CNTs; CNTs

1. Introduction

Hydrogen plays an important role in the energy sector. It is not only one of the most important feedstocks for the production of hydrocarbon fuels and chemicals, but also considered to be an ideal energy carrier for the renewable energy storage due to its high energy density and environmental friendliness [1,2]. However, hydrogen does not exist in its pure state in nature, like oxygen, and has to be produced from hydrogen-containing resources such as natural gas, coal, biomass and water by reforming, gasification, thermal decomposition or electrolysis. Currently, about 96% hydrogen is produced from fossil fuels [3,4]. The industrial processes produce significant amounts of CO_2, which is a major greenhouse gas (GHG) to cause global warming.

Hydrogen production from water splitting or electrolysis derived from renewable energy, such as solar (photovoltaic) or wind energy, is sustainable and provides an environmentally-friendly pathway to contribute towards meeting the constantly growing demand for energy supply and storage. For example, conversion of intermittent or excess solar (photovoltaic, PV) electrical energy into chemical energy by water electrolysis into hydrogen fuels can be used to store surplus solar energy during peak generation periods. During low generation periods (e.g., the night), these H_2 fuels can then be used to efficiently re-generate electricity via fuel cells. Fuel cells are energy conversion devices that electrochemically convert fuels such as hydrogen into electricity with high power density, high efficiency, and low GHG emissions [5]. Using H_2 as a fuel, the only by-product of the fuel cell reaction is water, which can be fed back into the water electrolysis process. Fig. 1 shows a schematic of the role of water electrolysis (electrochemical or photoelectrochemical types) and fuel cells in such environmentally-friendly energy solutions.

Unfortunately, water electrolysis is greatly constrained by the kinetically sluggish oxygen evolution reaction (OER) because it is thermodynamically and kinetically unfavorable for removing of four electrons to form oxygen–oxygen double bond [6]. Consequently, huge amount of efforts have been devoted to develop catalysts for more effective water electrolysis. Metal oxides, including RuO_2 and IrO_2-based electrodes [7–9], base metal

---

*Corresponding author.

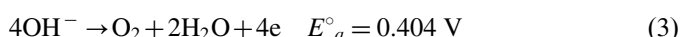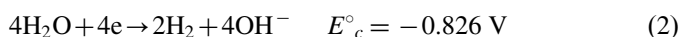*E-mail address:* s.jiang@curtin.edu.au (S.P. Jiang).

(Co, Fe, Ni, Mn) oxides [10,11] or hydroxides layers [12–14], spinels [15], and perovskites [16–18] have been intensively studied. One of the major disadvantages of metal oxides based catalysts is their relatively poor electrical conductivity. Carbon nanotubes (CNTs) possess high surface area, high conductivity and being corrosion resistant, providing an ideal platform to support the metal oxides for the development of efficient OER catalysts. CNTs based metal free catalysts also have been identified recently and showed the potential applications. In this review, we start with brief introduction to the basic principles in electrolysis, followed by the review of the key developments on metal oxides, metal oxide–CNTs hybrids and the CNTs based metal free OER catalysts.
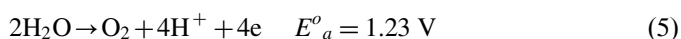
2. Water electrolysis reactions

Water electrolysis is the process of electrically splitting water into oxygen and hydrogen. The overall water electrolysis can be described by the following equation:
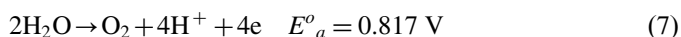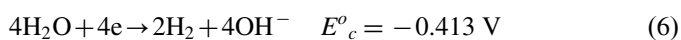
$$2H_2O \rightarrow 2H_2 + O_2 \tag{1}$$

The overall process is composed of hydrogen evolution reaction (HER) on the cathode and OER on the anode of the electrolyzer. Hence, in alkaline solutions (pH 14), the corresponding cathode and anode reactions are

$$4H_2O + 4e \rightarrow 2H_2 + 4OH^- \qquad E^\circ_c = -0.826 \text{ V} \tag{2}$$

$$4OH^- \rightarrow O_2 + 2H_2O + 4e \qquad E^\circ_a = 0.404 \text{ V} \tag{3}$$

where E°_c and E^o_a are the equilibrium half-cell potentials at standard conditions of 1 atm and 25 °C. In acid solutions (pH 0),

$$4H^+ + 4e \rightarrow 2H_2 \qquad E^o_c = 0.0 \text{ V} \tag{4}$$

$$2H_2O \rightarrow O_2 + 4H^+ + 4e \qquad E^o_a = 1.23 \text{ V} \tag{5}$$

In neutral conditions (pH 7), the reactions are

$$4H_2O + 4e \rightarrow 2H_2 + 4OH^- \qquad E^o_c = -0.413 \text{ V} \tag{6}$$

$$2H_2O \rightarrow O_2 + 4H^+ + 4e \qquad E^o_a = 0.817 \text{ V} \tag{7}$$

Thus at standard conditions, the equilibrium or reversible potential is 1.23 V for water electrolysis. The water electrolysis
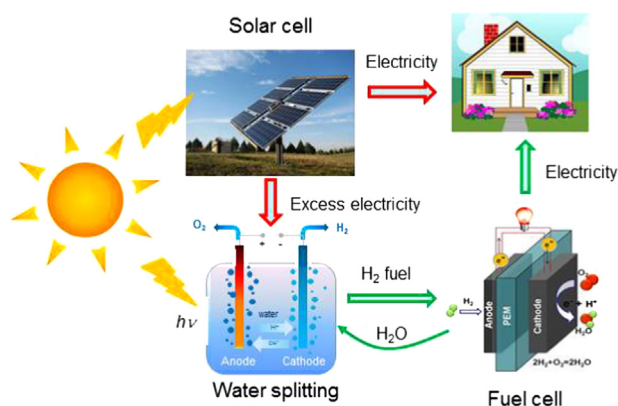

Fig. 1. Schematic representation of the energy cycle using water electrolysis to store excess solar electrical energy and fuel cells to provide the electricity during the low peak or night period.

is relatively favorable in acid and alkaline conditions due to the presence of deprotonated water molecules available for OER in alkaline solutions or HER in acid solutions. This also explains why water electrolysis in neutral condition is kinetically more difficult. In practice, production of hydrogen is hindered by the remarkable stability of water itself because the free energy required for the overall process of water electrolysis amounts to 237.21 kJ mol^{-1}.

3. Electrocatalysts for water electrolysis

3.1. Electrocatalysts for HER

Water electrolysis reaction includes two half-cell reactions, HER on the cathode and OER on the anode. The best materials for HER are noble metals: Pt, Pd, Rh or Ir. Trasatti investigated the HER in acid solution and observed a volcano-type dependence of the exchange currents for HER on the strength of intermediate metal–hydrogen (M–H) bond, of which Pt shows the best activity [19]. In order to reduce the noble metal loading, Kelly et al. synthesized HER electrocatalysts by supporting one monolayer of Pt on low-cost molybdenum carbide (Mo$_2$C) substrate. The monolayered Pt–Mo$_2$C thin film showed Pt-like HER activity while displaying excellent stability under HER conditions [20]. Sub-monolayer to monolayer of Pt supported on tungsten carbide (WC) allows for a significant decrease in Pt loading for HER [21]. Density functional theory (DFT) calculations and experimental measurements indicate that the monolayered Pt-WC surface exhibits chemical and electronic properties that are very similar to bulk Pt [22]. Low-cost electrocatalysts for HER with high activity have also been investigated and developed, including molybdenum disulfide MoS$_2$ [23,24], nanostructured WS$_2$ [25], nickel phosphide (Ni$_2$P) [26] and Cobalt phosphide (CoP) [27,28]. Recently, Zheng et al. reported a metal-free catalyst by coupling graphitic-carbon nitride (g-C$_3$N$_4$) with nitrogen-doped graphene [29]. This metal-free hybrid catalyst showed comparable electrocatalytic HER activity with the existing well-developed metallic catalysts, such as nanostructured MoS$_2$, but lower than that of the state-of-the-art Pt catalyst.

Compared with HER, OER is thermodynamically and kinetically unfavorable. Thus, considerable research efforts have been devoted to the development of OER catalysts with the aim of achieving high electrocatalytic activity and stability. In the following discussion, we will focus on the OER catalysts and particularly the role of CNTs for the development of advanced OER catalysts.

3.2. Electrocatalysts for OER

3.2.1. Noble metals and metal oxides

Similar to HER, in acid solutions, noble metal based on Ru, Ir, Pd, Pt, Au and their alloys are important OER catalysts [30–32]. Miles and Thomason studied systematically the OER in acid solutions (0.1 M H$_2$SO$_4$, 80 ± 2 °C) by cyclic voltammetry and showed that the order of OER activity is Ir ∼ Ru > Pd > Rh > Pt > Au > Nb > Zr ∼ Ti ∼ Ta (see Fig. 2) [31]. On the other hand, Danilovic et al. found that the most

active metal oxide is Os, and the order of activity for OER in acid media is Os»Ru > Ir > Pt»Au, but the stability of Os is low [32]. It has been reported that in the case of Ru, Ir and Pt and the corresponding carbon supported NPs, the OER activities of the oxidized metal catalysts are in the order of Ru > Ir > Pt[33].

First-row transition metal oxides such as Ni, Co, Mn and Fe have been widely studied for their relatively good activity for OER. Trotochaud et. al. prepared FeO_x, CoO_x NiO_x and MnO_x thin films with 2–3 nm by solution-cast and found that the activities for OER are in the order of $NiO_x > CoO_x > FeO_x > MnO_x$ [11]. Their catalytic activities for OER appear to be related to the $OH–M^{2+\delta}$ bond strength ($0 \leq \delta \leq 1.5$) with the order of $Ni < Co < Fe < Mn$[34], opposite to that of the activity. The M–O bond binding energy can also be tuned by alloying the metal oxides with other elements. Li et al. reported that doping Ni with Cu and Mn had adverse effect on the performance for OER, while addition of Co and Cr in Ni slightly increased the activity for OER, however, addition of Fe significantly increased the current density and lower the onset potential as well as the Tafel slope [35]. Diaz-Morales et al. studied Ni-based double hydroxides with Cr, Mn, Fe, Co, Cu, and Zn at the atomic scale and showed that doping $Ni(OH)_2$ with Cr, Mn, and Fe increased the catalytic activity of the Ni-based double hydroxides toward OER, while a deleterious effect was observed for the Co, Cu, and Zn doped $Ni(OH)_2$ (see Fig. 3) [36].

It has been known that the addition of Fe into nickel oxide and/or the formation of Fe–Ni alloys, Fe–Ni oxides/hydroxides reduce the overpotential for OER. Louie and Bell [37] conducted a detailed investigation on the electrochemical activity of electrodeposited Ni–Fe film for OER in alkaline solution. The results indicate that the interaction between Ni and Fe leads to an improvement of OER activity, and Ni–Fe film with a composition of 40%Fe exhibits OER activity that is ~2 orders of magnitude higher than that of a Ni film and ~3 orders of magnitude higher than that of a Fe film. Fig.4 shows the variation of the specific current density and the overpotential of Ni film as a function of the Fe composition [37]. Friebel et al. studied the mixed $Ni_{1-x}Fe_xOOH$ using operando X-ray absorption spectroscopy (XAS) and high energy resolution fluorescence detection and found that Fe^{3+} in $Ni_{1-x}Fe_xOOH$ occupies octahedral sites with unusually short Fe–O bond distances, induced by edge-sharing with surrounding $[NiO_6]$ octahedra [38]. Using computational methods, the authors established that this structural modification results in near optimal adsorption energies of OER intermediates and low overpotentials at Fe sites. By contrast, Ni sites in $Ni_{1-x}Fe_xOOH$ are not active for the oxidation of water [38].

Wang et al. recently showed that lithium-induced ultra-small $NiFeO_x$ nanoparticles (NPs) exhibited a high activity and stability for overall water electrolysis in alkaline solutions, achieving $10\ mA\ cm^{-2}$ current at 1.51 V for over 200 h without degradation in 1 M KOH, better than the iridium benchmark catalysts [39]. Delithiated $Li(NiFe)PO_4$ NPs anchored on reduced graphene oxide sheets also showed a good performance, generating a current density of 10 mA cm^{-2} at an overpotential of 0.27 V in 0.1 M KOH [40]. The high activity of delithiated $Li(NiFe)PO_4$ was considered as a
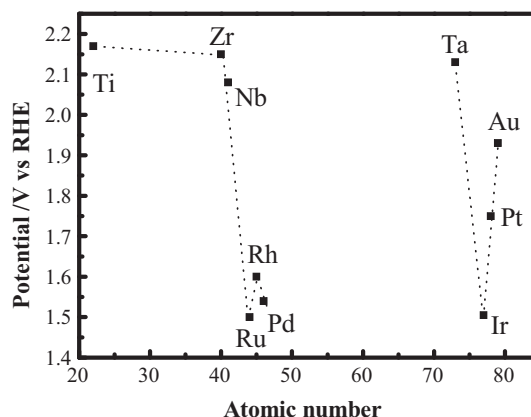

Fig. 2. Summary of cyclic voltammetric results for various metallic catalysts measured in 0.1 M H_2SO_4 at 80 °C. The potential vs. RHE is shown where the current density attains $2\ mA\ cm^{-2}$ using a potential sweep rate of $50\ mV\ s^{-1}$ (after Ref. [31]).

result of the significant increase of electrochemically active surface area (ECSA) and the increased oxidation state of the metal centers for delithiated $LiMPO_4$. The same group also found that electrochemically tuned cobalt–nickel–iron oxides from the corresponding sulfides grown directly on the carbon fiber electrodes exhibited a low overpotential of 0.23 V at $10\ mA\ cm^{-2}$ and good stability for over 100 h in 1 M KOH solution [41].

An effective catalyst active site is likely to contain multiple redox-active metal ions capable of buffering the multi-electron processes necessary for water oxidation. Studying complex oxide containing multi elements to screen optimized composition for OER is of great significance. Electrocatalytic OER response to metal stoichiometry in amorphous metal oxide films containing iron, cobalt, and nickel, formulated as a-$Fe_{100-y-z}Co_yNi_zO_x$ were systematically studied [42]. It was found that small concentration of iron produced a significant improvement in Tafel slopes, and cobalt or nickel was critical in lowering the onset potential. The best catalytic parameters of the series were obtained for the film with composition a-$Fe_{20}Ni_{80}$ [42]. Gerken et al. reported combinatorial screening of nearly 3500 trimetallic $A_xB_yC_zO_q$ mixed metal oxide compositions [43]. Using a fluorescence-based parallel screening method, the OER activity of catalyst arrays under alkaline conditions were directly detected, and the composition–activity relationships amongst mixed oxides composed of earth-abundant elements were determined. Significant sustained activity is observed only in the presence of Co or Ni, and the data draw attention to synergistic interactions between these redox-active ions and Lewis-acidic cations, such as Fe, Al, Ga, and Cr. The best activities were observed with oxides composed of Ni and Fe, together with another element, such as Ba, Ca, Cr and Sr [43].

3.2.2. Perovskite oxides

Perovskites with structure of ABO_3 is another class of OER catalysts that has been intensively investigated [16,44–46]. The physico-chemical and catalytic properties of perovskites can be
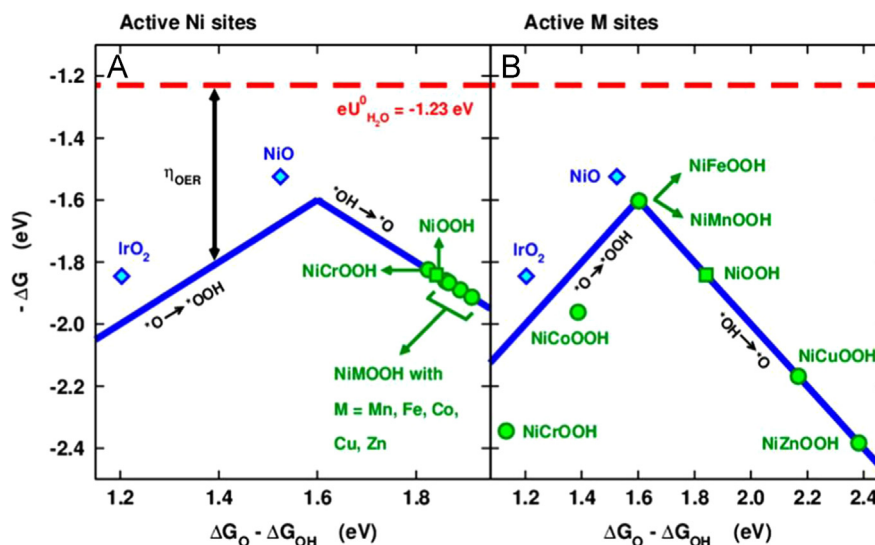
Fig. 3. Sabatier-type volcano plots for Ni-based oxyhydroxide sites doped with transition metals. The surfaces were doped with Cr, Mn, Fe, Co, Cu, and Zn. (a) Effect of doping on Ni sites. (b) Activity of dopants in a NiOOH lattice (after Ref. [36]).
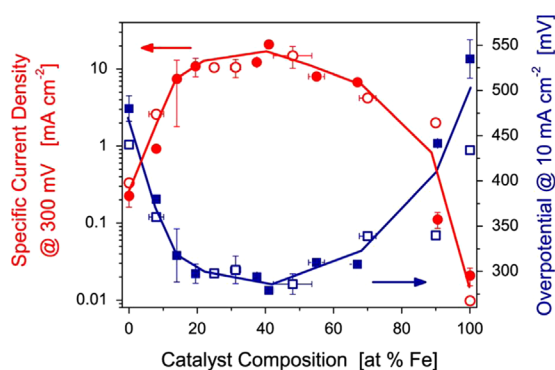

Fig. 4. Oxygen evolution activity of electrodeposited Ni–Fe catalysts, taken at $\eta = 300$ mV and 10 mA cm^{-2} specific current density, as a function of composition in 0.1 M KOH. Filled and open symbols correspond to the measurements taken using rotating and stationary Au working electrode substrates for which electrodeposited films are ~ 70 and ~ 25 nm thick, respectively (after Ref. [37]).

modified by substituting ions of the same or different oxidation states in the A and/or B sites. The OER electrocatalytic activities of substituted perovskite (A$_{1-x}$A$'_x$BO$_3$, where A is a lanthanide mainly La, A$'$ is an alkaline earth metal mainly Sr, and B is a first-row transition metal) were studied systematically [47]. Suntivich et al. proposed that the e_g filling of surface transition metal cations can greatly influence the binding of OER intermediates on the perovskites surface and thus the OER activity. The highest OER activity among all oxides studied as predicted by the e_g activity descriptor is Ba$_{0.5}$Sr$_{0.5}$Co$_{0.8}$Fe$_{0.2}$O$_{3-\delta}$ (BSCF), and the intrinsic OER activities of perovskites exhibit a volcano-shaped dependence on the occupancy of the 3d electron with an e_g symmetry of surface transition metal cations in an oxide, as shown in Fig. 5 [47]. Double perovskites (Ln$_{0.5}$Ba$_{0.5}$)CoO$_{3-\delta}$ (Ln=Pr, Sm, Gd and Ho) are also potentially active catalysts for the OER in alkaline solutions [18].

3.2.3. Carbon nanotube supported metal oxides

One of the practical issues associated with the application of metal oxides as electrocatalysts for water electrolysis is the relatively high resistance due to fact that most of the metal oxides are semiconductors with wide band gap or insulator [48]. One strategy is to combine the electronically conducting carbon materials such as CNTs with metal oxides. CNTs are seamless cylinders composed of one or more curved layers of graphene with either open or closed ends and have been extensively studied as supports for electrocatalysts due to the high surface area, high conductivity and good corrosion resistance. Metal oxides, such as NiO$_x$ [49–51], CoO$_x$ [52], MnO$_x$ [53] and NiFeO$_x$ [54] have been supported onto CNTs, showing promising activity and stability for OER. Wu et al. developed a hybrid consisting of Co$_3$O$_4$ nanocrystals supported on single-walled CNTs (SWNTs) simply by mixing Co$_3$O$_4$ with SWNTs in the presence of toluene. The Co$_3$O$_4$/SWNTs hybrid electrode for the OER exhibited a much enhanced catalytic activity as well as superior stability for OER under neutral and alkaline conditions compared with bare Co$_3$O$_4$, which only performed well in alkaline solution [52].

Due to the fact that the as-prepared CNTs are generally chemical inert, hence, it is necessary to modify or functionalize the surface of CNTs to introduce anchor sites for nucleating and anchoring metallic or metal oxide NPs. Generally, CNTs can be functionalized by covalent attachment of chemical groups through bonding to the π-conjugated skeleton of the CNTs or by non-covalent self-assembly or wrapping of functional polyelectrolytes or solvents. The covalent functionalization methods, including sidewall halogenation, hydrogenation, and radical additions and so on, have been intensively studied [55]. The most common covalent functionalization involves the attachment of carbonyl and hydroxyl groups via an acid oxidation treatment with a mixture of HNO$_3$/H$_2$SO$_4$ or by plasma etching [56,57]. Unfortunately, the distribution of carbonyl and carboxyl groups generated by acid treatment was not controllable and inhomogeneous, and would
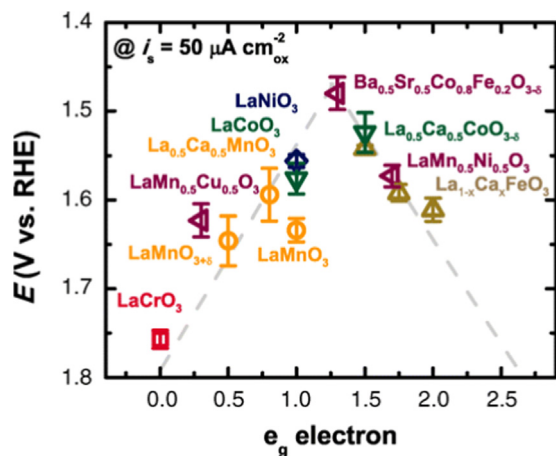
Fig. 5. Relation between the OER catalytic activity, defined by the over-potentials at 50 μA cm_{ox}^{-2} of OER current, and the occupancy of the e_g-symmetry electron of the transition metal (B in ABO_3). Data symbols vary with type of B ions (Cr, red; Mn, orange; Fe, beige; Co, green; Ni, blue; mixed compounds, purple), where $x=0$, 0.25, and 0.5 for Fe. Error bars are based on at least three independent measurements. The dashed volcano lines are shown for guidance only (after Ref. [47]).

lead to the aggregation of NPs [58]. Acid oxidation introduces structural defects and disrupts the delocalized π electron system in the CNT sidewalls, consequently altering the electronic and mechanical properties to a degree that may significantly affect the performance of the electrocatalysts.

An important issue of metal oxide–CNTs hybrids is to functionalize CNTs with a suitable degree of functional groups for nucleating and anchoring nanocrystals without damaging the electronic properties. Dai group developed a modified Hummers oxidation method to produce mild oxidized CNTs, which provided sufficient anchoring sites for the nucleation and growth of metal oxides [59]. Lu and Zhao synthesized a Co_3O_4/CNT hybrid through a facile mild oxidation and hydrothermal precipitation two-step approach. The hybrid catalyst exhibited an onset potential of 1.51 V *vs.* RHE and an overpotential of 0.39 V at a current density of 10 mA cm^{-2} [60]. Mildly oxidized CNTs are advantageous for introducing oxygen containing functional groups for anchoring of high catalytic active Co_3O_4 NPs and at the same time maintaining structural integrity for efficient charge transport. Ultrathin nickel–iron layered double hydroxide (LDH) nanoplates supported on mildly oxidized CNTs achieved a current density of 10 A g^{-1} at $\eta=0.228$ V in 1 M KOH with catalysts loading of 0.25 mg cm^{-2} (see Fig. 6) [54]. Growth of LDH nanoplates on the functional groups on CNTs contributed to the high OER activity of the NiFe-LDH/CNT complexes [54].

Development of more effective functionalization method that can not only introduce high density and homogeneous surface functional groups but also has little or no structural damage to CNTs is attracting increasing interests. Non-covalent functionlization of CNTs by various surfactants [57], aromatic compounds [57,61], and functional polymers [62,63] has been intensively studied as such functionalization method is effective to introduce high density and uniform active sites with little detrimental effect on CNTs. NiO_x NPs with size around 2–3 nm supported on

polyethylenimine (PEI) functionalized CNTs exhibited high activities for OER, achieving a current density of 100 A g^{-1} at an overpotential of 0.35 V due to the synergistic effect between NiO_x and CNTs [51].

CNTs can be synthesized by using transitional metals, such as Fe, Co, Ni, Au, Pd, Ag, Pb, Mn, Cr, Ru, Mo, Cu, under controlled conditions [64]. Hence, incorporating metal catalysts during the growth of CNTs could be effective to develop OER electrocatalysts with high activity and structural stability. Based on this concept, our group developed metal–CNTs hybrids with sufficiently high metal oxide catalyst loading synthesized by arc-discharge and chemical vapor deposition (CVD) methods as electrocatalysts for OER in alkaline solutions, as shown in Fig. 7 [65]. The metal–CNTs hybrids produced by arc-discharge (M-CNTs-Arc) and CVD (M-CNTs-CVD) exhibit a core–shell-like structure, in which metal NPs encapsulated by graphene shells are connected by CNTs, forming M-CNTs network hybrids. M-CNTs-Arc has $NiCo_{0.16}Fe_{0.34}$ metal core and shows very high activity and superior stability for OER, achieving 100 A g^{-1} at an over-potential (η) of 0.29 V and 500 A g^{-1} at $\eta=0.37$ V in 1 M KOH solution. This is probably the highest activity reported for OER in alkaline solutions. The advantages of this one-pot metal–CNTs hybrid synthesis method provides a strong inter-action between the in situ formed metal oxide NPs and CNTs, is also easy scalable and allows the encapsulation of metal NPs inside the CNTs or graphene shells, achieving highly active and stable metal–CNTs hybrids for OER [65]. Table 1 compares some of the best metal oxide–CNTs hybrid OER catalysts reported in the literature.

Doping CNTs with heteroatoms such as nitrogen, boron and sulfur can significantly modify the absorption strength and electron structure of CNTs, which in turn can tune their overall catalytic activity, selectivity and durability [67–69]. Wang et al. synthesized cobalt-embedded nitrogen doped CNTs using cobalt–phthalocyanine (Co-Pc) as a precursor and the sources of cobalt and nitrogen [70]. The as-synthesized catalysts showed current density of 50 mA cm^{-2} in alkaline media and 10 mA cm^{-2} in neutral media at an overpotential of 0.30 V. Li et al. synthesized Co_3O_4 nanocrystals embedded in N-doped mesoporous graphitic carbon layer/CNT hybrids by a facile carbonization and subsequent oxidation process of CNT-based metal–organic frameworks (MOFs) and achieved an onset potential of 1.50 V vs. RHE and an overpotential of 0.32 V at 10 mA cm^{-2} in alkaline solution [71]. Park et al. developed a facile one-pot synthetic method to prepare $La_{0.5}Sr_{0.5}Co_{0.8}Fe_{0.2}O_3$ (LSCF)-nitrogen-doped carbon nanotube composite catalyst combining a simple calcination synthesis for LSCF NPs and injection chemical vapor deposition for the N-CNTs and showed good bi-functionality for the ORR and the OER [72].

3.2.4. CNTs based metal free catalysts

Recently, heteroatom doped carbon materials have been investigated as potential metal free OER catalysts. Zhao et al. synthesized a nitrogen-doped carbon material for OER in alkaline media, achieving a current density of 10 mA cm^{-2}
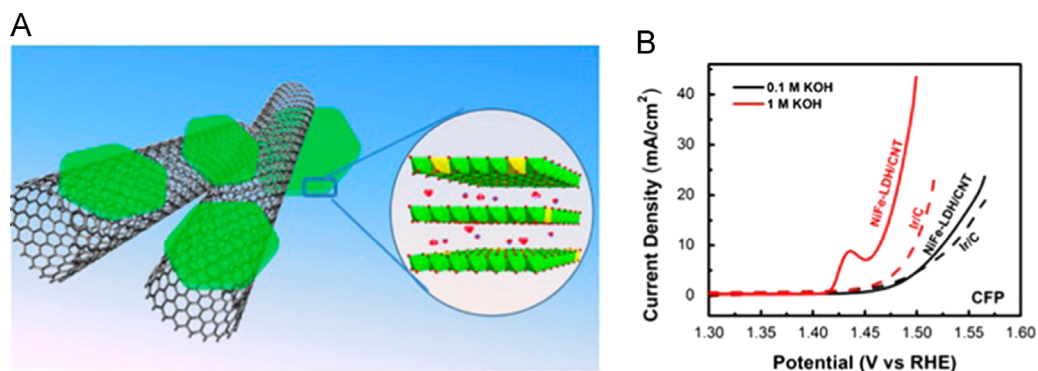
Fig. 6. (A) Schematic showing the NiFe-LDH/CNT hybrid architecture and NiFe-LDH crystal structure; (B) Polarization curves of NiFe-LDH/CNT hybrid and Ir/C in 0.1 M and 1 M KOH solution (after Ref. [54]).
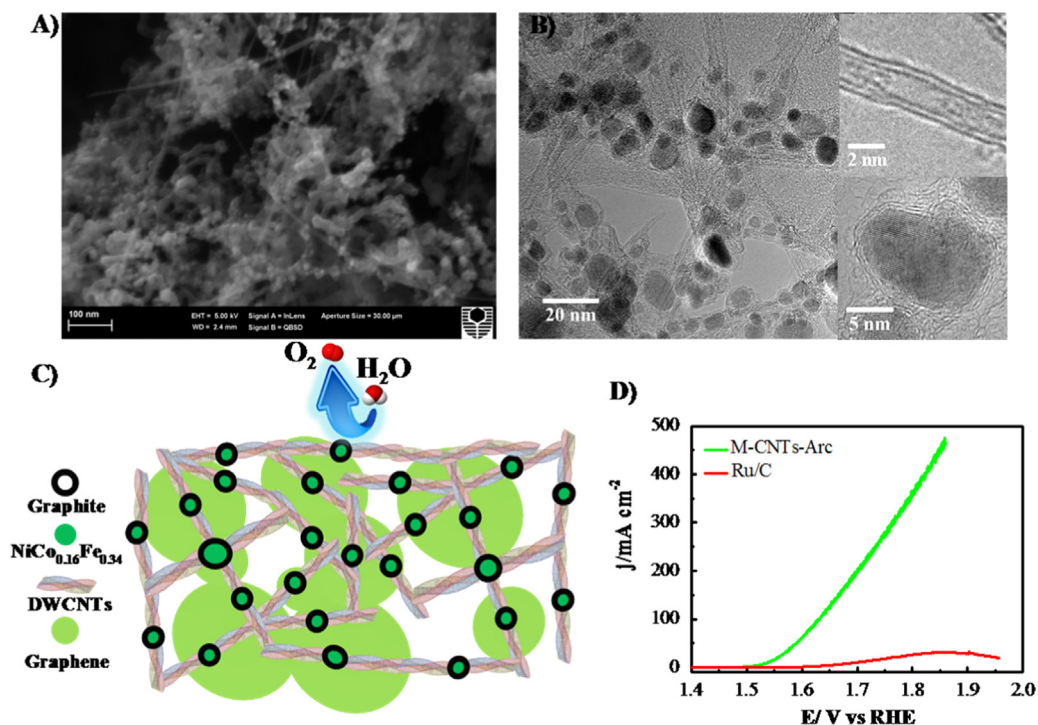

Fig. 7. (A) SEM and (B) TEM images of metal–CNTs hybrid synthesized by arc-discharge (M-CNTs-Arc). The inset in (B) shows a double-walled CNT and metal core with graphene shell, (C) scheme showing the M-CNTs-Arc hybrid, and (D) polarization curves of M-CNTs-Arc and benchmark catalyst Ru/C (after Ref. [65]).

Table 1
List of the selected best CNTs or carbon fiber supported OER catalysts reported in the literature.

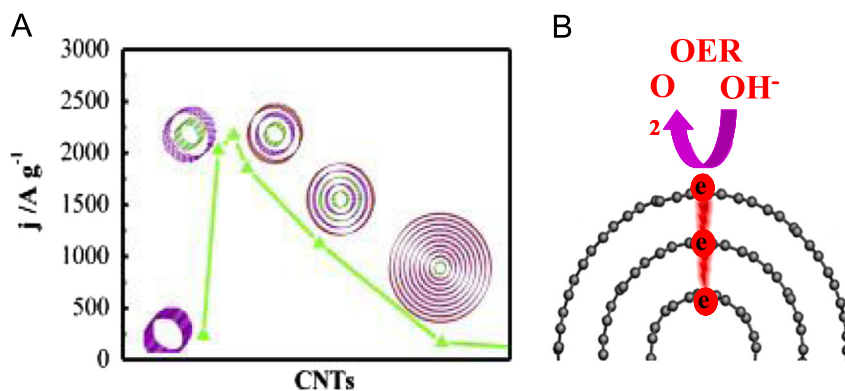| Materials	Test condition		Onset potential	Potential	References
	Electrolyte	Loading (mg cm^{-2})	(V)	V @J_{10}	
NiFe-LDH/CNT	1 M KOH	0.25	1.45	1.485	[54]
ECT-Co$_{0.37}$Ni$_{0.26}$Fe$_{0.37}$O	1 M KOH	–	–	1.462	[41]
M-CNTs-Arc	1 M KOH	0.025	1.48	1.52	[65]
NiFeO$_x$/CFP	1 M KOH	1.6	1.43	1.46	[39]
De-LNiFeP/rGO	0.1 M KOH	0.5	1.45	1.51	[40]
	1 M KOH		-	1.41	
20%Ir/C	0.1 M KOH		1.5	1.545	
	1 M KOH		1.5	1.52	
Echo-MWCNTs	0.1 M KOH	1	–	1.68	[66]
	1 M KOH		–	1.59	

Fig. 8. (A) Plot of the activity of CNTs for the OER in 1 M KOH solution as a function of number of walls. The mass specific activity was measured at 1.8 V (vs RHE) at scan rate of 1 mV s^{-1} and rotating rate of 2000 rpm with CNTs loading of 0.025 mg cm^{-2}; (B) scheme showing the electron tunneling effect for the OER on triple-walled CNTs (after Refs. [80,81]).

at an overpotential of 0.38 V [73]. The results indicated that the high OER activity of the nitrogen-doped carbon materials was originated from the pyridinic-nitrogen- or/and quaternary-nitrogen-related active sites [73]. Tian et al. reported the synthesis of N-doped graphene/SWNTs hybrid for both ORR and OER and observed a current density of 10 mA cm^{-2} at a potential of 1.63 V for OER [74]. Graphitic carbon nitride (g-C$_3$N$_4$) hybridized with CNTs was synthesized using cyanamide as precursor and the optimal CNT content was found to be ~0.2 wt% in the composite, which displayed a 2.4-fold enhancement in photocatalytic water splitting over pure g-C$_3$N$_4$ [75]. Graphitic carbon nitride nanosheets and CNTs composites exhibited high activity and stability for OER [76]. Chen et al. reported the synthesis of N,O-dual doped graphene-CNT hydrogel film electrocatalyst via layer-by-layer assembly of chemically converted graphene (with intrinsic oxygen impurities) and CNTs through a simple filtration procedure followed by N-doping with ammonia [77]. This self-supported material showed high OER activity, which has been attributed with the dual active-sites mechanism originating from the synergy of chemically converted graphene and CNTs [77].

In addition of heteroatom doped CNTs, modification of the CNT structure can create active sites for electrochemical reactions such as ORR. Li et al. demonstrated that partially unzipping the "few-walled CNTs" via oxidation and high temperature reaction with ammonia, creating nanoscale sheets of graphene attached to the inner tubes, can act as ORR catalysts in both acid and alkaline conditions [78]. The inner walls remain intact and retain their electrical conductivity, which facilitates charge transport during electrocatalysis. Waki et al. found that the formation of topological defects on the MWNTs through successive oxidation by refluxing in sulfuric acid and concentrated nitric acid and annealing in argon at high temperature can significantly enhance the activity for ORR in acid solutions compared with pristine CNTs [79]. Such structurally modified CNTs could also be effective for OER.

Most recently, we have found that CNTs composed of 2–3 concentric tubes had an outstanding activity for the OER in alkaline solution as compared with SWNTs and MWNTs [80]. For example, current density measured at 1.8 V (vs RHE) for the OER on triple-walled CNTs is 56 mA cm^{-2}, ~10 times

higher than 5.9 mA cm^{-2} measured on SWNTs and 35 times higher than 1.6 mA cm^{-2} measured on MWNTs. One hypothesis is that for the OER on CNTs with 2–3 inner tubes or walls, efficient electron transfer occurs on the inner tubes of the CNTs most likely through electron tunneling between outer wall and inner tubes, significantly promoting the charge transfer reaction of OER at the surface of outer wall of the CNTs [80,81]. For SWNTs, such separation of functionality for OER is not possible, while effective electron tunneling between outer wall and inner tubes of the CNTs diminishes as the number of walls increases due to the reduced dc bias (i.e., the driving force) across the walls or layers of MWNTs (see Fig. 8) [81].

4. Conclusions and perspectives

One of the critical issues in the development of water electrolysis technologies is the kinetically sluggish OER. Thus, the development of more efficient, structurally durable and economically viable electrocatalysts for OER is urgently needed. In acid solution, noble metals and their oxides are still the most effective electrocatalysts. However, in alkaline solution, electrocatalysts based on the transition metal oxides/hydroxides such as Co, Ni, Fe systems have been demonstrated as the most active and low cost OER catalysts. Perovskite or double perovskite oxides also showed promising potential as highly efficient electrocatalysts for OER in alkaline solutions. The disadvantages of the generally low electrical conductivity of metal oxides can be partly overcome by forming metal oxide–CNTs hybrids. The most attractive strategy appears to be the *in situ* incorporation of metal oxide catalysts in the synthesis of CNTs as shown in [65]. The attractiveness of such one-pot metal–CNTs hybrid synthesis method is the high stability of the graphene shell encapsulated metal oxide NPs and easy scalability for mass production.

Metal free OER catalysts are gaining increasing attention and offer exciting opportunities for the development of new generation electrocatalysts for water electrolysis, particularly in the areas of heteroatom doped CNTs and graphene materials. The recent discovery of the outstanding electrocatalytic activity of CNTs with 2–3 inner tubes or walls [80,81] opens a new dimension in the development of highly effective and

inherently stable CNTs based electrocatalysts for OER by manipulating the quantum properties of carbon materials. However, the origin of the OER activity of such CNTs-based metal-free catalysts has not been fully understood yet, and more efforts are urgently needed to fundamentally understand the origin of the active sites and the charge transfer process between the outer and inner tubes by the electron tunneling mechanism under the water electrolysis conditions.

Acknowledgment

References

[1] G. Gahleitner, Int. J. Hydrogen Energy 38 (2013) 2039–2061.
[2] S.H. Jensen, P.H. Larsen, M. Mogensen, Int. J. Hydrogen Energy 32 (2007) 3253–3257.
[3] M. Balat, Int. J. Hydrogen Energy 33 (2008) 4013–4029.
[4] M.N. Manage, D. Hodgson, N. Milligan, S.J.R. Simons, D.J.L. Brett, Int. J. Hydrogen Energy 36 (2011) 5782–5796.
[5] S.P. Jiang, X. Wang, Fuel cells: advances and challenges, in: V.V. Kharton (Ed.), Handbook of Solid State Electrochemistry, vol. II, Wiley-VCH, 2011, pp. 179–264 Chapter 5.
[6] T.J. Meyer, Nature 451 (2008) 778–779.
[7] J.C. Cruz, V. Baglio, S. Siracusano, V. Antonucci, A.S. Arico, R. Ornelas, L. Ortiz-Frade, G. Osorio-Monreal, S.M. Duron-Torres, L.G. Arriaga, Int. J. Electrochem. Sci. 6 (2011) 6607–6619.
[8] A. Di Blasi, C. D'Urso, V. Baglio, V. Antonucci, A.S. Arico, R. Ornelas, F. Matteucci, G. Orozco, D. Beltran, Y. Meas, L.G. Arriaga, J. Appl. Electrochem. 39 (2009) 191–196.
[9] H. Dau, C. Limberg, T. Reier, M. Risch, S. Roggan, P. Strasser, Chemcatchem 2 (2010) 724–761.
[10] C. Bocca, A. Barbucci, M. Delucchi, G. Cerisola, Int. J. Hydrogen Energy 24 (1999) 21–26.
[11] L. Trotochaud, J.K. Ranney, K.N. Williams, S.W. Boettcher, J. Am. Chem. Soc. 134 (2012) 17253–17261.
[12] R.L. Doyle, M.E.G. Lyons, Phys. Chem. Chem. Phys. 15 (2013) 5224–5237.
[13] D. Cibrev, M. Jankulovska, T. Lana-Villarreal, R. Gomez, Int. J. Hydrogen Energy 38 (2013) 2746–2753.
[14] R.L. Doyle, M.E.G. Lyons, J. Electrochem. Soc. 160 (2013) H142–H154.
[15] F. Cheng, J. Shen, B. Peng, Y. Pan, Z. Tao, J. Chen, Nat. Chem. 3 (2011) 79–84.
[16] K.J. May, C.E. Carlton, K.A. Stoerzinger, M. Risch, J. Suntivich, Y.L. Lee, A. Grimaud, Y. Shao-Horn, J. Phys. Chem. Lett. 3 (2012) 3264–3270.
[17] S. Raabe, D. Mierwaldt, J. Ciston, M. Uijttewaal, H. Stein, J. Hoffmann, Y.M. Zhu, P. Blochl, C. Jooss, Adv. Funct. Mater. 22 (2012) 3378–3388.
[18] A. Grimaud, K.J. May, C.E. Carlton, Y.-L. Lee, M. Risch, W.T. Hong, J. Zhou, Y. Shao-Horn, Nat. Commun. 4 (2013).
[19] S. Trasatti, J. Electroanal. Chem. Interfacial Electrochem. 39 (1972) 163–184.
[20] T.G. Kelly, K.X. Lee, J.G. Chen, J. Power Sources 271 (2014) 76–81.
[21] D.V. Esposito, S.T. Hunt, A.L. Stottlemyer, K.D. Dobson, B.E. McCandless, R.W. Birkmire, J.G. Chen, Angew. Chem. Int. Ed. 49 (2010) 9859–9862.
[22] D.V. Esposito, J.G. Chen, Energy Environ. Sci. 4 (2011) 3900–3912.
[23] T.F. Jaramillo, K.P. Jørgensen, J. Bonde, J.H. Nielsen, S. Horch, I. Chorkendorff, Science 317 (2007) 100–102.
[24] J. Kibsgaard, Z. Chen, B.N. Reinecke, T.F. Jaramillo, Nat. Mater. 11 (2012) 963–969.
[25] D. Voiry, H. Yamaguchi, J. Li, R. Silva, D.C.B. Alves, T. Fujita, M. Chen, T. Asefa, V.B. Shenoy, G. Eda, M. Chhowalla, Nat. Mater. 12 (2013) 850–855.
[26] E.J. Popczun, J.R. McKone, C.G. Read, A.J. Biacchi, A.M. Wiltrout, N. S. Lewis, R.E. Schaak, J. Am. Chem. Soc. 135 (2013) 9267–9270.
[27] E.J. Popczun, C.G. Read, C.W. Roske, N.S. Lewis, R.E. Schaak, Angew. Chem. Int. Ed. 53 (2014) 5427–5430.
[28] J. Tian, Q. Liu, A.M. Asiri, X. Sun, J. Am. Chem. Soc. 136 (2014) 7587–7590.
[29] Y. Zheng, Y. Jiao, Y. Zhu, L.H. Li, Y. Han, Y. Chen, A. Du, M. Jaroniec, S.Z. Qiao, Nat. Commun. 5 (2014).
[30] J.C. Cruz, A. Ramos Hernandez, M. Guerra-Balcazar, A.U. Chavez-Ramirez, J. Ledesma-Garcia, L.G. Arriaga, Int. J. Electrochem. Sci. 7 (2012) 7866–7876.
[31] M.H. Miles, M.A. Thomason, J. Electrochem. Soc. 123 (1976) 1459–1461.
[32] N. Danilovic, R. Subbaraman, K.-C. Chang, S.H. Chang, Y.J. Kang, J. Snyder, A.P. Paulikas, D. Strmcnik, Y.-T. Kim, D. Myers, V. R. Stamenkovic, N.M. Markovic, J. Phys. Chem. Lett. 5 (2014) 2474–2478.
[33] T. Reier, M. Oezaslan, P. Strasser, ACS Catal. 2 (2012) 1765–1772.
[34] R. Subbaraman, D. Tripkovic, K.-C. Chang, D. Strmcnik, A.P. Paulikas, P. Hirunsit, M. Chan, J. Greeley, V. Stamenkovic, N.M. Markovic, Nat. Mater. 11 (2012) 550–557.
[35] X. Li, F.C. Walsh, D. Pletcher, Phys. Chem. Chem. Phys. 13 (2011) 1162–1167.
[36] O. Diaz-Morales, I. Ledezma-Yanez, M.T.M. Koper, F. Calle-Vallejo, ACS Catal. (2015) 5380–5387.
[37] M.W. Louie, A.T. Bell, J. Am. Chem. Soc. 135 (2013) 12329–12337.
[38] D. Friebel, M.W. Louie, M. Bajdich, K.E. Sanwald, Y. Cai, A.M. Wise, M.-J. Cheng, D. Sokaras, T.-C. Weng, R. Alonso-Mori, R.C. Davis, J. R. Bargar, J.K. Nørskov, A. Nilsson, A.T. Bell, J. Am. Chem. Soc. 137 (2015) 1305–1313.
[39] H. Wang, H.-W. Lee, Y. Deng, Z. Lu, P.-C. Hsu, Y. Liu, D. Lin, Y. Cui, Nat. Commun. 6 (2015).
[40] Y. Liu, H. Wang, D. Lin, C. Liu, P.-C. Hsu, W. Liu, W. Chen, Y. Cui, Energy Environ. Sci. 8 (2015) 1719–1724.
[41] W. Chen, H. Wang, Y. Li, Y. Liu, J. Sun, S. Lee, J.-S. Lee, Y. Cui, ACS Cent. Sci. 1 (2015) 244–251.
[42] R.D.L. Smith, M.S. Prévot, R.D. Fagan, S. Trudel, C.P. Berlinguette, J. Am. Chem. Soc. 135 (2013) 11580–11586.
[43] J.B. Gerken, S.E. Shaner, R.C. Masse, N.J. Porubsky, S.S. Stahl, Energy Environ. Sci. 7 (2014) 2376–2382.
[44] J.-I. Jung, H.Y. Jeong, J.-S. Lee, M.G. Kim, J. Cho, Angew. Chem. Int. Ed. 53 (2014) 4582–4586.
[45] S. Raabe, D. Mierwaldt, J. Ciston, M. Uijttewaal, H. Stein, J. Hoffmann, Y. Zhu, P. Blöchl, C. Jooss, Adv. Funct. Mater. 22 (2012) 3378–3388.
[46] M. Risch, A. Grimaud, K.J. May, K.A. Stoerzinger, T.J. Chen, A. N. Mansour, Y. Shao-Horn, J. Phys. Chem. C. 117 (2013) 8628–8635.
[47] J. Suntivich, K.J. May, H.A. Gasteiger, J.B. Goodenough, Y. Shao-Horn, Science 334 (2011) 1383–1385.
[48] J. Jiang, Y. Li, J. Liu, X. Huang, C. Yuan, X.W. Lou, Adv. Mater. 24 (2012) 5166–5180.
[49] X. Yu, T. Hua, X. Liu, Z. Yan, P. Xu, P. Du, ACS Appl. Mater. Interfaces 6 (2014) 15395–15402.
[50] X. Zhou, Z. Xia, Z. Zhang, Y. Ma, Y. Qu, J. Mater. Chem. A 2 (2014) 11799–11806.
[51] Y. Cheng, P.K. Shen, S.P. Jiang, Int. J. Hydrogen Energy 39 (2014) 20662–20670.
[52] J. Wu, Y. Xue, X. Yan, W. Yan, Q. Cheng, Y. Xie, Nano Res. 5 (2012) 521–530.
[53] K. Mette, A. Bergmann, J.-P. Tessonnier, M. Hävecker, L. Yao, T. Ressler, R. Schlögl, P. Strasser, M. Behrens, Chemcatchem 4 (2012) 851–862.
[54] M. Gong, Y. Li, H. Wang, Y. Liang, J.Z. Wu, J. Zhou, J. Wang, T. Regier, F. Wei, H. Dai, J. Am. Chem. Soc. 135 (2013) 8452–8455.
[55] D. Tasis, N. Tagmatarchis, A. Bianco, M. Prato, Chem. Rev. 106 (2006) 1105–1136.
[56] Z.Q. Tian, S.P. Jiang, Y.M. Liang, P.K. Shen, J. Phys. Chem. B 110 (2006) 5343–5350.
[57] L. Meng, C. Fu, Q. Lu, Prog. Nat. Sci. 19 (2009) 801–810.
[58] S. Wang, X. Wang, S.P. Jiang, Langmuir 24 (2008) 10505–10512.
[59] Y. Liang, Y. Li, H. Wang, H. Dai, J. Am. Chem. Soc. 135 (2013) 2013–2036.
[60] X. Lu, C. Zhao, J. Mater. Chem. A 1 (2013) 12053–12059.

[61] S. Murugesan, K. Myers, V. Subramanian, Appl. Catal. B-Environ. 103 (2011) 266–274.

[62] Y.L. Hsin, K.C. Hwang, C.-T. Yeh, J. Am. Chem. Soc. 129 (2007) 9999–10010.

[63] S. Wang, S.P. Jiang, X. Wang, Nanotechnology 19 (2008).

[64] J.-P. Tessonnier, D.S. Su, Chemsuschem 4 (2011) 824–847.

[65] Y. Cheng, C. Liu, H.M. Cheng, S.P. Jiang, Acs Appl. Mater. Interfaces 6 (2014) 10089–10098.

[66] X. Lu, W.-L. Yim, B.H.R. Suryanto, C. Zhao, J. Am. Chem. Soc. 137 (2015) 2901–2907.

[67] L. Yang, S. Jiang, Y. Zhao, L. Zhu, S. Chen, X. Wang, Q. Wu, J. Ma, Y. Ma, Z. Hu, Angew. Chem. -Int. Ed. 50 (2011) 7132–7135.

[68] Q. Shi, F. Peng, S. Liao, H. Wang, H. Yu, Z. Liu, B. Zhang, D. Su, J. Mater. Chem. A 1 (2013) 14853–14857.

[69] J. Zhu, S.P. Jiang, R. Wang, K. Shi, P.K. Shen, J. Mater. Chem. A 2 (2014) 15448–15453.

[70] Z. Wang, S. Xiao, Z. Zhu, X. Long, X. Zheng, X. Lu, S. Yang, ACS Appl. Mater. Interfaces 7 (2015) 4048–4055.

[71] X. Li, Y. Fang, X. Lin, M. Tian, X. An, Y. Fu, R. Li, J. Jin, J. Ma, J. Mater. Chem. A 3 (2015) 17392–17402.

[72] H.W. Park, D.U. Lee, M.G. Park, R. Ahmed, M.H. Seo, L.F. Nazar, Z. Chen, Chemsuschem 8 (2015) 1058–1065.

[73] Y. Zhao, R. Nakamura, K. Kamiya, S. Nakanishi, K. Hashimoto, Nat. Commun. 4 (2013).

[74] G.-L. Tian, M.-Q. Zhao, D. Yu, X.-Y. Kong, J.-Q. Huang, Q. Zhang, F. Wei, Small 10 (2014) 2251–2259.

[75] Y.L. Chen, J.H. Li, Z.H. Hong, B. Shen, B.Z. Lin, B.F. Gao, Phys. Chem. Chem. Phys. 16 (2014) 8106–8113.

[76] T.Y. Ma, S. Dai, M. Jaroniec, S.Z. Qiao, Angew. Chem. Int. Ed. 53 (2014) 7281–7285.

[77] S. Chen, J. Duan, M. Jaroniec, S.-Z. Qiao, Adv. Mater. 26 (2014) 2925–2930.

[78] Y. Li, W. Zhou, H. Wang, L. Xie, Y. Liang, F. Wei, J.C. Idrobo, S. J. Pennycook, H. Dai, Nat. Nanotechnol. 7 (2012) 394–400.

[79] K. Waki, R.A. Wong, H.S. Oktaviano, T. Fujio, T. Nagai, K. Kimoto, K. Yamada, Energy Environ. Sci. 7 (2014) 1950–1958.

[80] Y. Cheng, C.W. Xu, L.C. Jia, J.D. Gale, L.L. Zhang, C. Liu, P.K. Shen, S.P. Jiang, Appl. Catal. B -Environ. 163 (2015) 96–104.

[81] Y. Cheng, J. Zhang, S.P. Jiang, Chem. Commun. (Camb.) 51 (2015) 13764–13767.

Dr. San Ping Jiang obtained his BEng from South China University of Technology and Ph.D. from The City University, London. He is a Professor at the Department of Chemical Engineering and Deputy Director of Fuels and Energy Technology Institute, Curtin University, Australia and Adjunct Professor of the University of Sunshine Coast University, Australia. Before joining Curtin University in 2010, Dr. Jiang worked at Essex University in UK, CSIRO Materials Science and Manufacturing Division, Ceramic Fuel Cells Ltd. in Australia and Nanyang Technological University in Singapore. His research interests encompass fuel cells, electrolyzers, supercapacitors, electrocatalysis and nano-structured functional materials.